

# Journal of Materials Chemistry C

Accepted Manuscript



This is an *Accepted Manuscript*, which has been through the Royal Society of Chemistry peer review process and has been accepted for publication.

*Accepted Manuscripts* are published online shortly after acceptance, before technical editing, formatting and proof reading. Using this free service, authors can make their results available to the community, in citable form, before we publish the edited article. We will replace this *Accepted Manuscript* with the edited and formatted *Advance Article* as soon as it is available.

You can find more information about *Accepted Manuscripts* in the [Information for Authors](#).

Please note that technical editing may introduce minor changes to the text and/or graphics, which may alter content. The journal's standard [Terms & Conditions](#) and the [Ethical guidelines](#) still apply. In no event shall the Royal Society of Chemistry be held responsible for any errors or omissions in this *Accepted Manuscript* or any consequences arising from the use of any information it contains.

# Crystallization-enhanced emission through hydrogen-bond interactions in blends containing hydroxyl-functionalized azine and poly(4-vinyl pyridine)

Tai-Shen Hsiao, Shiang-Lin Deng, Ke-Ying Shih and Jin-Long Hong\*

*Department of Materials and Optoelectronic Science, National Sun Yat-Sen University,*

*Kaohsiung 804214, Taiwan*

An organic azine derivative of CN4OH, containing both of the *para*- and the *ortho*-hydroxyl (*o*- and *p*-OH) groups, is a fluorescent material with its emission efficiency dependent on the degree of crystallinity. With inherent hydroxyl groups, CN4OH can be homogeneously blended with different amounts of poly(4-vinyl pyridine) (PVP) through intermolecular hydrogen-bond (H-bond) interactions. With the incorporations of one and two molar equivalents of PVP, the solid CN4OH/PVP(4/1) and (2/1) blends emit strongly with intensity larger than the pure CN4OH. Nevertheless, further increase of the PVP content considerably reduced the crystallinity and the emission efficiency of the blend. Initially, PVP was preferably H-bonded to the *p*-OHs of CN4OH, resulting in the beneficial crystallization-enhanced emission (CEE); nevertheless, the PVP added in the later step started to bond to the *o*-OHs of CN4OH, reducing the crystallinity and the CEE-related fluorescence. With appropriate H-bond interaction, the CN4OH/PVP(2/1) blend emits with a high quantum yield ( $\Phi_F$ ) of 88%, in contrast to the low  $\Phi_F$  of 15% for pure CN4OH.

## Introduction

Since the first report on silole derivative<sup>1,2</sup> with aggregation-induced emission (AIE) property in 2001, lots of organic and polymeric materials<sup>3-8</sup> have been prepared and characterized to emit with the unusual AIE or aggregation-enhanced emission (AEE) characters. By forming suspended aggregates in the solution state, the AIE-active fluorophores emitted with much larger intensity compared to the weakly (or non-) emissive solution state. It is generally accepted that the restricted intramolecular rotation (RIR) of the phenyl peripheries<sup>9,10</sup> against the central silole core, which reduces the possible nonradiative decay channels and leads to enhanced emission, is the main mechanism responsible for the intense emission in the aggregated state. With this respect, large substituents had been linked to the AIE-active cores for the sake of introducing efficient rotational restriction on the AIE-active fluorophores.

In many of the AIE systems, crystallization<sup>11-16</sup> is the main cause for its enhanced emission. Fluorophores with crystallization-induced and -enhanced emission (CIE and CEE) behaviors are highly-emissive when in the crystalline state but are weakly or non-emissive when in the amorphous aggregated form. In amorphous aggregates, there exist molecular voids and large free volumes that may allow free molecular rotation. However, in the crystalline phase, fluorophores molecules are fastened by the crystalline lattice and restriction forces imposed by the crystalline lattice are so efficient that fluorescent molecules in the crystalline lattice are no longer free to rotate, resulting in emission intensity much higher than that in the amorphous state.

The noncovalent H-bond interactions were used frequently to intensify RIR on the AIE-active fluorophores. The dimer structure of AIE-active 2,7-bis(4-(*tert*-butylthio)phenyl)uorenone<sup>17</sup> (BPU) was effectively locked by intermolecular H-bonds and the excited BPU underwent enhanced excimer emission

with fewer non-radiative decay pathways. The salicylideneaniline<sup>18</sup> compound formed a gel in certain organic solvents and its AEE behavior is ascribed to the formation of *J*-aggregates and the inhibition of molecular rotation by H-bond interactions in the viscous gel. Other compounds with hydrazine,<sup>19</sup> benzoxazole,<sup>20</sup> acrylamido<sup>21</sup> and naphthalide<sup>22</sup> functions were also reported to show enhanced emission in the gelled states promoted by H-bond interactions. Besides the small-mass fluorophores, poly(fluorene-*alt*-naphthol)<sup>23</sup> (PFN) prepared in our laboratory was also found to be AEE-active due to the restricted molecular rotation promoted by inter and intrachain H-bond interactions. The restricted molecular rotation of PFN can be further reinforced by blending it with poly(*N*-vinyl pyrrolidone)<sup>24</sup> (PVR). The resulting PFN/PVR blends showed enhanced emission due to the facile intermolecular H-bond interactions. AIE-active molecules with pyridine and triphenylamine terminals<sup>25,26</sup> were blended with poly(vinyl phenol) and poly(vinyl alcohol) to generate *pseudo*-linear polymer or *pseudo*-crosslinked network blends with higher emission intensity compared to the pure fluorophore itself.

Study on organic imine (C=N) compounds is also good example to illustrate the effect of conformational restriction on the emission behavior of organic fluorophores. The C=N isomerization in the excited state was known as the predominant decay pathway for imine dyes with an unbridged C=N bond and so the imine compounds are often nonfluorescent.<sup>27-29</sup> By inhibiting the C=N isomerization, certain heterocyclic compounds containing covalently-bridged C=N are therefore fluorescent materials. The C=N isomerization was also used as signal system by inhibiting C=N isomerization through complexation of a guest species<sup>30-38</sup> (mostly, metal ions) to a sophisticatedly designed luminescent-sensing molecule. Besides the above-mentioned examples, H-bond interaction was also applied to suppress the undesired C=N isomerization in the excited state. The salicylaldehyde azine derivative of CN4OH

(Scheme 1) illustrates how the C=N isomerization can be effectively inhibited by intramolecular H-bond interaction between the *ortho*-hydroxyl group and the imino nitrogen atom within the *pseudo* six-membered enolimine ring. The CN4OH is therefore AEE-active emitter<sup>39</sup> whereas analogous azine derivatives without the *o*-OH groups are not fluorophores at all.

With inherent H-bond donating hydroxyl groups, CN4OH can be thoroughly blended with poly(4-vinyl pyridine) (PVP) containing H-bond accepting pyridine side groups (Scheme 1). Hypothetically, molecular rotation of CN4OH should be efficiently locked by the viscous polymeric chains of PVP and fluorescence of the blends should be increased with increasing PVP content in the blends. However, no simple correlation was found in our research. The CN4OH/PVP blends are actually crystalline materials with their solid-state emission properties strongly related to the degree of crystallinity and the H-bonding pattern of the blends. Crystalline packing of the CN4OH molecules in the blends was affected by the H-bonding pattern, which in turn was complicated by the fact that the pyridinyl ring of PVP can bond to either the *para*- or the *ortho*-hydroxyl (*o*- or *p*-OH) groups of CN4OH. As illustrated in Scheme 1, when H-bonding is between the *p*-OH of CN4OH and pyridinyl ring of PVP (route i), parallel array of CN4OH molecules is the favorable crystalline form existing in the blends. Fluorophore molecules are fastened by the crystalline lattice and the fluorescent molecules of CN4OH in the crystalline blends are no longer free to rotate, resulting in the enhanced emission of the blends. On the other hand, if the intermolecular H-bonding between PVP and the *o*-OH group of CN4OH occurs (route ii), fluorescence of the corresponding blend will be largely reduced because the intervening PVP segments will laterally bond to CN4OH, interrupting the crystalline packing of the CN4OH molecules. Besides, the *pseudo* six-membered enolimine ring, originally held by the intramolecular H-bonding between *o*-OH and imino nitrogen

atom, will be ruptured and the liberated C=N bond will undergo isomerizes in the excited state to result in emission quenching. The difference caused by H-bonding to *p*- or *o*-OH groups is so significant that our experimental results indicated that the quantum yields ( $\Phi_F$ ) of the CN4OH/PVP blends can be tuned from 22 to 88%, dependent on the amounts of PVP applied in the blends. To distinguish the difference between *p*- and *o*-OH groups, analogous molecule of CN2OH with *o*-OH groups was also prepared and blended with PVP to prepare model blends for study. The resulting CN2OH/PVP blends showed the detrimental H-bonding effect due to the sole H-bonding to the *o*-OH groups. The relationship between H-bond interactions and crystallization-enhanced emission (CEE) is the focus of this study and experimental results following this manuscript verifies it.

## Experimental Section

### Materials

Synthetic procedures and characterization data of CN4OH and CN2OH were given in the supporting information. P4VP ( $M_w \sim 22,000$ , Aldrich chem. Co.) was used directly without purification.

### Instrumentation

$^1\text{H}$  NMR spectra were recorded with a Varian Unity Inova-500 MHz FT-NMR instrument. Tetramethylsilane (TMS) was used as the internal standard. The molar masses of the organic molecules were determined by a Bruker Autoflex III MALDI/TOF mass spectrometer. PL emission spectra were obtained from a LabGuide X350 fluorescence spectrophotometer using a 450 W Xe lamp as the continuous light source. The composition of the sample was analyzed by a Heraus CHN-OS rapid element analyzer with acetanilide and benzoic acid as standards. A quartz cell with

dimensions of 0.2 x 1.0 x 4.5 cm<sup>3</sup> was used for the PL emission spectra measurements. Stock solutions of the organic and polymeric fluorophores with a concentration of 10<sup>-3</sup> M in THF (or DMSO) were first prepared. Aliquots of these stock solutions were transferred to 10 mL volumetric flasks, into which appropriate volumes of THF (or DMSO) and water were added dropwise under vigorous stirring to furnish 10<sup>-4</sup> M solutions with different water contents from 0 to 90 v%. PL emission spectroscopy was immediately performed once the solutions were prepared. Solid samples were prepared by drop-casting sample solutions over quartz plates. For solvent-fuming treatment, the sample plates were placed in close channel saturated ethanol vapor. Fluorescence quantum yields ( $\Phi_F$ ) of the solution mixtures with varied compositions were determined by comparison with a quinine sulfate standard. An integrating sphere was used for the film sample. The wide-angle X-ray diffraction (WAXD) pattern of the solid blend was obtained from a Siemens D5000 diffractometer. Particle sizes of the aggregates in solution were measured by dynamic light scattering (DLS) using a Brookhaven 90 plus spectrometer equipped with a temperature controller. An argon ion laser operating at 658 nm was used as the light source.

## Results and discussion

The small-mass fluorophore of CN4OH was prepared from condensation reaction between hydrazine and 2,4-dihydroxyl benzaldehyde. The solid CN4OH is a good emitter although it only emits dimly in the solution state. As we will discuss later, the fluorescence of the solid CN4OH is attributed to its crystal structure in view that better crystals from solvent-fuming process emitted with higher emission intensity than the as-synthesized CN4OH of lower crystallinity. The as-synthesized CN4OH was then blended with different amounts of PVP to result in CN4OH/PVP (x/y) blends (x/y: molar ratio between the OH donating and the pyridinyl accepting groups)

with different crystallinity and emission efficiency. It is suggested that effective rotational restriction imposed by the crystal lattice is crucial for the strong solid-state emission of CN4OH. To compare, CN2OH/PVP (1/2) blend was also prepared to clarify the role of H-bonding on the crystallization-related fluorescence. Before discussion on the complicated blend system, the fluorescence properties of the pure CN4OH need to be evaluated in the first place.

### **Emission behavior of CN4OH**

Solution emission spectra of CN4OH in solvent mixtures gave the emission response upon aggregation. As illustrated in Figure 1A, dilute solutions ( $10^{-4}$  M) of CN4OH in THF exhibited discernible emission at 530 nm and increasing water content in the solution gradually increased the emission intensity. Solution containing 90 v% of water emitted with intensity more than twice to the pure solution of CN4OH in THF. Aggregates formed upon water addition are responsible for the observed emission enhancement. Aggregated particles formed in the mixture solutions can be characterized by dynamic light scattering (DLS) measurement. The summarized result in Figure 1B revealed a trend that aggregated particles formed in the mixture solution shrunk in sizes when the water content in the solution was increased. Nanoparticles formed in THF/water (v/v = 7/3) solution are large in dimensions (with the average hydrodynamic diameter ( $D_h$ ) around 240 nm). Increasing water content in the solution resulted in smaller particles ( $D_h = 120$  nm for the THF/water (v/v = 1/9) solution). Molecular rotation of CN4OH is supposed to be more effectively restricted within the confined spaces of a smaller particle because of the large steric constraint given by the congested environment; thus, the non-radiative decay channels can be more effectively blocked to result in the intensified fluorescence in the mixture solutions. Smaller nanoparticles formed in solutions containing more water are therefore more



emissive than larger aggregates in solution with less water.

Although discernible, the emissions shown in the spectra of Figure 1A are still very weak. In contrast to the weakly-emissive solution state, the solid CN4OH is a good emitter with a measured quantum yield ( $\Phi_F$ ) of 15%. It has been previously reported that the emission intensity of a CEE-active solid<sup>26,39,40</sup> can be largely increased by solvent-fuming process. To demonstrate the CEE character of CN4OH, we therefore conducted solvent-fuming procedures on CN4OH and used it to demonstrate the merits of solvent-induced crystallinity on the fluorescence efficiency. Emission spectra of the as-synthesized CN4OH in an atmosphere saturated with ethanol vapor were then recorded (Figure 2A). The emission intensity of CN4OH was gradually enhanced with increasing exposure time under ethanol vapor. The emission efficiency of the fumed films can be quantized by the measured  $\Phi_{FS}$ : the initial  $\Phi_F$  of 15% for the as-synthesized CN4OH can be raised to 32% after 40 min exposure under ethanol vapor.

WAXD spectra can be used to evaluate the effect of solvent-fuming on crystallinity of CN4OH. The as-synthesized CN4OH is semi-crystalline materials with few small diffraction peaks over the large amorphous background (Figure 2B). After solvent-fuming, crystallinity of CN4OH was greatly enhanced in view of the larger crystalline to amorphous peak ratio. The crystallinity of CN4OH can be largely increased by solvent-fuming (from 38% to 64%) after 40 min exposure under ethanol vapor. Effective rotational restriction in a perfectly-arrayed crystalline lattice therefore led to the enhanced emission of the fumed CN4OH. We can then conclude that CN4OH is a CEE-active fluorophore with its emission efficiency strongly dependent on its crystallinity. Also, the rigid enolimine rings, maintained by the intramolecular H-bonding, should be well preserved in the crystalline state in order to prevent the unfavorable C=N isomerization in the excited state.

### Blending of CN4OH with PVP

Initially, the possible H-bond interaction between CN4OH and PVP was investigated in the solution state. However, the solution emission spectra of CN4OH and CN4OH/PVP (2/1) mixtures (Figure 3A) in DMSO are essential the same, showing no effect from the addition of PVP component. In the dilute solution ( $[CN4OH] = 10^{-4}$  M), the minor solute molecules of CN4OH and PVP should be well separated by the majority of the DMSO solvent media, thereby, intermolecular H-bond interactions between distant CN4OH molecules and PVP chains were absent in the solution. Without intermolecular H-bond interactions, solution emission of the CN4OH/PVP (2/1) mixtures is essentially the same with the pure CN4OH solution. However, the situation can be altered by confining both CN4OH and PVP in small aggregated nanoparticles, within which close contacts and facile H-bond interactions are possible, generated by adding water into the pure DMSO solution. The emission intensity of the CN4OH/PVP (2/1) mixtures can be largely increased by adding water into the solution. The emission enhancement is also correlated with the size variations detected by DLS measurements (Figure 3B). In the solution containing 30 v% of water, mixtures of CN4OH/PVP (2/1) formed large particles ( $D_h \sim 500$  nm) with broad size distribution whereas adding water resulted in particles with smaller sizes ( $D_h$  ranged from 300 to 440 nm) and narrower size distribution. The facile H-bond interactions present in the small particles will impose effective restriction on the molecular motions of CN4OH, leading to the emission enhancement for the blend solutions with high water content.

In distinct to the solution samples, the emission behavior of the solid CN4OH is directly related to the amounts of PVP in the blends. Primarily, stoichiometric consideration was required when emission spectra of the solid blends was measured.

As the first and the second equivalents of the H-bond accepting pyridinyl ring were added in the respective CN4OH/PVP (4/1) and CN4OH/PVP (2/1) blends, we observed emission enhancement (Figure 4A). The emission intensity of the solid CN4OH/PVP (2/1) blend is more than 7-fold to that of the solid CN4OH. The composition-related emission behavior of the CN4OH/PVP blends indicated that the added PVP should be homogeneously mixed with CN4OH in order to exert the continuous emission enhancement. As similar to the aggregated solutions of the CN4OH/PVP (2/1) mixtures (cf. Figure 3A), effective H-bond interactions between the solid CN4OH and PVP should exist in the blends in order to exert the composition-dependent fluorescence behavior. Molecular rotation of CN4OH molecules should be effectively restricted by viscous polymer chains to result in the observed enhanced emission in Figure 4A. However, the intensity gain was only observed in the initial blends of CN4OH/PVP(4/1) and (2/1). Further increase of the PVP content in CN4OH/PVP (1/1) only lowered the emission intensity. All the spectral variations described here can be best supported by the  $\Phi_F$  values listed in Table 1. With appropriate molar ratio between the H-bond donating and accepting groups, the CN4OH/PVP(2/1) blend is a highly-emissive material with a high  $\Phi_F$  value of 88% but the high content of PVP in CN4OH/PVP(1/1) caused the large reduction of  $\Phi_F$  to a low value of 22%.

Considering the stoichiometric amounts used in the blends, we suggested that certain fractions of the PVP components in the blend of CN4OH/PVP (1/1) may participate in the H-bond interaction to the *o*-OH groups of CN4OH, resulting in the lowering of the fluorescence. CN2OH molecule containing the *o*-OH groups was therefore prepared and was used to blend with PVP to prepare CN2OH/PVP (1/1) and (1/2) blends for identifying the detrimental bonding from the PVP-bonded *o*-OH groups. The solid-state emission spectra of CN2OH/PVP (1/1) and (1/2) blends were

compared with solid CN2OH in Figure 4B. The pure CN2OH emitted strongly but inclusion of PVP lowered the emission. Equivalent amounts of PVP in CN2OH/PVP(1/1) resulted in the slight decrease of the emission intensity but more significant emission reduction was observed when large excess of PVP was used in the CN2OH/PVP(1/2) blend. Variations of the emission intensity can be reflected from the measured quantum efficiency that pure CN2OH has a  $\Phi_F$  value of 21% (Table 1) and the added PVP reduced  $\Phi_F$  from 21 to 12%. We therefore suggested that intermolecular H-bond interaction between PVP and *o*-OHs of CN2OH (and CN4OH) is the main mechanism responsible for the reduced emissions of the CN2OH/PVP and the CN4OH/PVP (1/1) blends.

H-bonding to the *p*- and *o*-OH groups may cause varied crystallization behavior in the blends. Correlation between H-bond interaction and crystalline structure can be made by the WAXD spectra. With the incorporation of the amorphous PVP, the CN4OH/PVP(x/y) blends formed crystal with the main crystalline diffraction peaks (Figure 5A) at positions the same with those in the solvent-fumed CN4OH. In respect to the ratio between the crystalline peaks and amorphous background, we concluded that the CN4OH/PVP (2/1) blend has the highest crystallinity of 87% among all samples. Initially, addition of PVP tends to enhance crystallization of CN4OH molecules in the blends of CN4OH/PVP (4/1) and (2/1) but further increase of PVP content to CN4OH/PVP(1/1) resulted in the reduction of crystallinity. Variation on crystallinity of the blends is in line with the emission intensity of the blends, indicating that main factor controlling the emission efficiency is the crystallinity of the fluorescent CN4OH in the blends. For CN2OH system, the added PVP also decreased the crystallinity for the blends (Figure 5B). The lowering of the crystallinity is also correlated with the reduction on the fluorescence.

The *p*- and *o*-OH groups of CN4OH should have different H-bonding capability

towards the pyridinyl ring of PVP. For CN4OH, the intramolecular H-bonding in the enolimine ring stabilizes the *o*-OH groups, which are considered to be less reactive toward H-bonding to the externally-added PVP. In blends containing less amounts of PVP (i.e. CN4OH/PVP(4/1) and (2/1)), the added PVP chains tend to H-bond to the *p*-OH groups of CN4OH molecules but when large amounts of PVP are present in the blend of CN4OH/PVP(1/1), H-bonding to the stable *o*-OH groups of CN4OH started to take place. As illustrated in Scheme 1 (route i), the preferable H-bond interaction between the less-hindered *p*-OH groups of CN4OH and the pyridinyl ring of the PVP chains resulted in a molecular architecture with the polymeric PVP chains separated by the nearly-parallel crystalline arrays of CN4OH molecules. The intermolecular  $\pi$ - $\pi$  interactions between the neighboring phenyl rings of CN4OH molecules also facilitated the nearly-parallel arrangement of the CN4OH molecules, thus, CN4OH molecules in close vicinities packed to form crystalline domain responsible for the sharp WAXD peaks observed in Figure 5A. Within the crystalline lattices, molecular rotation of CN4OH was effectively restricted, leading to the high quantum yield ( $\Phi_F = 88\%$ ) of the CN4OH/PVP (2/1) blend. Also, despite lower in the content of the fluorescent CN4OH, the CN4OH/PVP (2/1) blend emitted with higher efficiency than CN4OH/PVP(4/1) containing higher fraction of fluorescent CN4OH. Therefore, the decisive factor leading to the high emission of the blends relies on the restricted molecular rotation, rather than the content, of the fluorophore.

Further increase of PVP content in CN4OH/PVP(1/1) resulted in the lowering of the fluorescence intensity. The reduced fluorescence of the CN4OH/PVP(1/1) is attributed to the rupture of the rigid enolimine ring and the decrease of the crystallinity. Besides H-bonding to the *p*-OH groups of CN4OH, the large amounts of PVP applied in CN4OH/PVP (1/1) started to compete with the imino nitrogen for the the *o*-OH groups of CN4OH. When the intermolecular H-bond interactions occurred,

the PVP chains will take over the H-bond originally existing in the enolimine ring and liberate the C=N bond. Upon photo-irradiation, the non-bonded C=N bond in the excited state will isomerizes to result in the emission quenching. Certain fractions of the PVP-bonded *o*-OH groups are responsible for the emission reduction observed in the CN4OH/PVP (1/1) blend. In addition to the rupture of the *pseudo* enolimine ring, the added PVP chains also caused the lowering of crystallinity for the CN4OH/PVP (1/1). As illustrated in Scheme 1 (route ii), once H-bonded to the *o*-OHs of the CN4OH molecules, chain segments of PVP will penetrate into the molecular spaces of the CN4OH molecules and interrupt their ordered crystalline packing, resulting in the lowering of the crystallinity. The molecular motion of the CN4OH molecules in the destructed amorphous domains was less restricted as compared to when CN4OH molecules were in the ordered crystalline lattice. Therefore, the CN4OH/PVP (1/1) blend with lower crystallinity will emit with less emission efficiency compared to CN4OH/PVP(2/1) with higher crystallinity (with the measured  $\Phi_F$  of 22 vs. 88%). Similar results can be also obtained in the CN2OH/PVP blends that H-bond interactions between the *o*-OH groups of CN2OH and PVP lowered the crystallinity and the emission efficiency (with the measured  $\Phi_F$  from 22 to 14%).

The results of this study indicate that molecular rotation of organic azine derivative can be efficiently restricted in the crystalline lattice. By application of appropriate H-bond interaction, crystallinity of the flurophores in the blend can be largely increased to produce highly-emissive materials. However, detrimental H-bond interaction resulted in the disordered fluorescent domains, within them non-radiative decay pathways through rotational motion in the excited state led to the reduced emission of the blends. Relationship between H-bond interaction and crystalline-enhanced emission can be thus evaluated in this study.

## Conclusion

The azine derivative of CN4OH is a crystalline material with its emission intensity dependent on the degree of crystallinity. By solvent-fuming, crystallinity of the CN4OH can be increased to result in crystals with higher emission intensity. Therefore, CN4OH is a fluorophore with the CEE character.

Through facile H-bond interactions with PVP, CN4OH formed homogeneous blends with different amounts of PVP. Most of the PVP component in the CN4OH/PVP (4/1) and (2/1) blends are H-bonded to the *p*-OH groups of CN4OH, helping formation of crystals with high emission efficiency. The CN4OH/PVP (2/1) blend is a highly-emissive crystal with a large  $\Phi_F$  value of 88%. Further increase of PVP content to CN4OH/PVP (1/1) resulted in the reduction of crystallinity and emission efficiency ( $\Phi_F = 22\%$ ). With the inevitable H-bonding to the *o*-OH groups of CN4OH, large amounts of PVP chains in CN4OH/PVP blend ruptured the rigid enolimine ring and liberated the C=N bond to undergo isomerization in the excited state, resulting in the reduced emission of the blend. The detrimental effect from the H-bonded *o*-OH groups can be also seen in the CN2OH/PVP blend. With preferable H-bond interactions to the *o*-OH groups of CN2OH, PVP acted to reduce the strong fluorescence of CN2OH.

## Acknowledgements

We appreciate the financial support from National Science Council, Taiwan, under the contract no. NSC 102-2221-E-110-084-MY3.

## References

- 1 J. Luo, Z. Xie, J. W. Y. Lam, L. Cheng, H. Chen, C. Qiu, H. S. Kwok, X. Zhan, Y. Liu, D. Zhu and B. Z. Tang, *Chem. Commun.*, 2001, 1740.

- 2 B. Z. Tang, X. Zhan, G. Yu, P. P. S. Lee, Y. Liu and D. Zhu, *J. Mater. Chem.*, 2001, **11**, 2974.
- 3 Aggregation-Induced Emission: Fundamentals
- 4 J. Liu, J. W. Y. Lam and B. Z. Tang, *J. Inorg. Organomet. Polym.*, 2009, **19**, 249.
- 5 Y. Hong, J. W. Y. Lam and B. Z. Tang, *Chem. Commun.*, 2009, 4332.
- 6 J. Wu, W. Liu, J. Ge, H. Zhang and P. Wang, *Chem. Soc. Rev.*, 2011, **40**, 3483.
- 7 Y. Hong, J. W. Y. Lam and B. Z. Tang, *Chem. Soc. Rev.*, 2011, **40**, 5361.
- 8 A. Qin, J. W. Y. Lam and B. Z. Tang, *Prog. Polym. Sci.*, 2012, **37**, 182.7.
- 9 J. Chen, C. C. W. Law, J. W. Y. Lam, Y. Dong, S. M. F. Lo, I. D. Williams, D. Zhu and B. Z. Tang, *Chem. Mater.*, 2003, **15**, 1535.
- 10 B. Z. Tang, Y. Geng, J. W. Y. Lam, B. Li, X. Jing, X. Wang, F. Wang, A. B. Pakhomov and X. Zhang, *Chem. Mater.*, 1999, **11**, 1581.
- 11 Z. Li, Y. Dong, B. Mi, Y. Tang, M. Haeussler, H. Tong, Y. Dong, J. W. Y. Lam, Y. Ren, H. H. Y. Sung, K. S. Wong, P. Gao, I. D. Williams, H. S. Kwok and B. Z. Tang, *J. Phys. Chem. B*, 2005, **109**, 10061.
- 12 Y. Dong, J. W. Y. Lam, A. Qin, J. Sun, J. Liu, Z. Li, J. Sun, H. H. Y. Sung, I. D. Williams, H. S. Kwok and B. Z. Tang, *Chem. Commun.*, 2007, 3255.
- 13 Y. Dong, J. W. Y. Lam, A. Qin, J. Liu, Z. Li, B. Z. Tang, J. Sun and H. S. Kwok, *Appl. Phys. Lett.*, 2007, **91**, 011111.
- 14 H. Tong, Y. Dong, M. Haeussler, J. W. Y. Lam, H. H. Y. Sung, I. D. Williams, J. Sun and B. Z. Tang, *Chem. Commun.*, 2006, 1133.
- 15 Y. Dong, J. W. Y. Lam, A. Qin, Z. Li, J. Sun, H. H. Y. Sung, I. D. Williams and B. Z. Tang, *Chem. Commun.*, 2007, 40.
- 16 H. Tong, Y. Dong, Y. Hong, M. Haeussler, J. W. Y. Lam, H. H. Y. Sung, X. Yu, J. Sun, I. D. Williams, H. S. Kwok and B. Z. Tang, *J. Phys. Chem. C*, 2007, **111**, 2287.
- 17 Y. Liu, X. Tao, F. Wang, J. Shi, J. Sun, W. Yu, Y. Ren, D. Zou and M. Jiang, *J.*



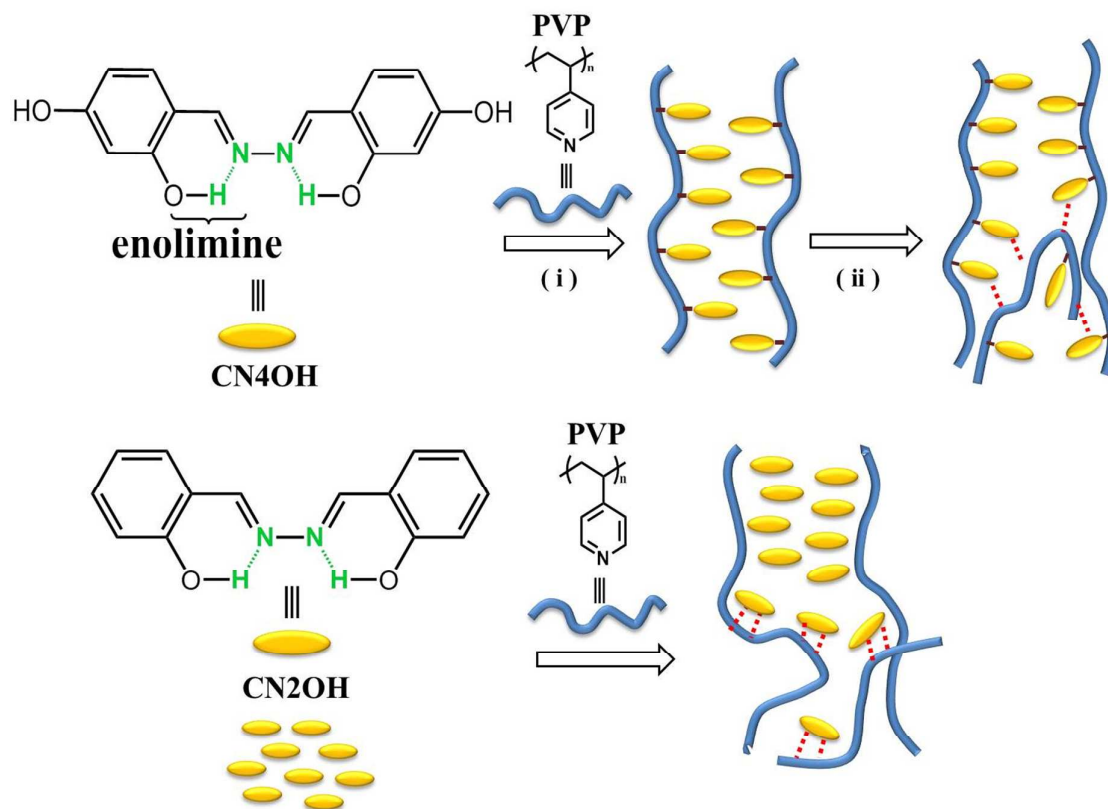
- Phys. Chem. C*, 2007, **111**, 6544.
- 18 P. Chen, R. Lu, P. Xue, T. Xu, G. Chen and Y. Zhao, *Langmuir*, 2009, **25**, 8395.
- 19 P. Zhang, H. Wang, H. Liu and M. Li, *Langmuir*, 2010, **26**, 10183.
- 20 T. H. Kim, M. S. Choi, B. H. Sohn, S. Y. Park, W. S. Lyoo and T. S. Lee, *Chem. Commun.*, 2008, 2364.
- 21 J. H. Wan, L. Y. Mao, Y. B. Li, Z. F. Li, H. Y. Qiu, C. Wang and G. Q. Lai, *Soft Matter*, 2010, **6**, 3195.
- 22 M. K. Nayak, *J. Photochem. Photobiol., A*, 2011, **217**, 40.
- 23 R. H. Chien, C. T. Lai and J. L. Hong, *J. Phys. Chem. C*, 2011, **115**, 12358.
- 24 R. H. Chien, C. T. Lai and J. L. Hong, *J. Phys. Chem. C*, 2011, **115**, 20732.
- 25 W. L. Chien, C. M. Yang, T. L. Chen, S. T. Li and J. L. Hong, *RSC Adv.*, 2013, **3**, 6930.
- 26 S. L. Deng, T. L. Chen, W. L. Chien and J. L. Hong, *J. Mater. Chem. C*, 2014, **2**, 651.
- 27 G. Q. Yang, F. Morlet-Savary, Z. K. Peng, S. K. Wu and J. P. Fouassier, *Chem. Phys. Lett.*, 1996, **256**, 536.
- 28 Z. M. Li and S. K. Wu, *J. Fluoresc.*, 1997, **7**, 237.
- 29 P. F. Wang and S. K. Wu, *J. Photochem. Photobiol., A*, 1995, **86**, 109.
- 30 J. S. Wu, W. M. Liu, X. Q. Zhuang, F. Wang, P. F. Wang, S. L. Tao, X. H. Zhang, S. K. Wu and S. T. Lee, *Org. Lett.*, 2007, **9**, 33.
- 31 W. M. Liu, L. W. Xu, R. L. Sheng, P. F. Wang, H. P. Li and S. K. Wu, *Org. Lett.*, 2007, **9**, 3829.
- 32 D. Ray and P. K. Bharadwaj, *Inorg. Chem.*, 2008, **47**, 2252.
- 33 J. R. Sheng, F. Feng, Y. Qiang, F. G. Liang, L. Sen and F. H. Wei, *Anal. Lett.*, 2008, **41**, 2203.
- 34 Z. X. Li, M. M. Yu, L. F. Zhang, M. Yu, J. X. Liu, L. H. Wei and H. Y. Zhang,

- Chem. Commun.*, 2010, **46**, 7169.
- 35 V. Chandrasekhar, P. Bag and M. D. Pandey, *Tetrahedron*, 2009, **65**, 9876.
- 36 H. S. Jung, K. C. Ko, J. H. Lee, S. H. Kim, S. Bhuniya, J. Y. Lee, Y. Kim, S. J. Kim and J. S. Kim, *Inorg. Chem.*, 2010, **49**, 8552.
- 37 N. Zhao, Y. H. Wu, R. M. Wang, L. X. Shi and Z. N. Chen, *Analyst*, 2011, **136**, 2277.
- 38 N. Zhao, Y. H. Wu, J. Luo, L. X. Shi, and Z. N. Chen, *Analyst*, 2013, **138**, 894.
- 39 L. Qian, B. Tong, J. Shen, J. Shi, J. Zhi, Y. Dong, F. Yang, Y. Dong, J. W. Y. Lam, Y. Liu and B. Z. Tang, *J. Phys. Chem. B*, 2009, **113**, 9098.
- 40 C. M. Yang, I. W. Lee, T. L. Chen, W. L. Chien and J. L. Hong, *J. Mater. Chem. C*, 2013, **1**, 2842.

**Table 1** Quantum yield ( $\Phi_F$ )<sup>a</sup> and crystallinity<sup>b</sup> of CN4OH, CN4OH/PVP(x/y) blends, CN2OH and CN2OH/PVP(x/y) blends.

<b>A. CN4OH/PVP(x/y) system</b>				
<b>x/y =</b>	1/0	4/1	2/1	1/1
<b><math>\Phi_F</math> (%)</b>	15	50	88	22
<b>Crystallinity (%)</b>	38	71	87	58
<b>B. CN2OH/PVP(x/y) system</b>				
<b>x/y =</b>	1/0	1/1	1/2	
<b><math>\Phi_F</math> (%)</b>	21	18	12	
<b>Crystallinity (%)</b>	88	78	71	

<sup>a</sup> determined from integrating sphere.<sup>b</sup> determined from WXDA spectra.



**Scheme 1** Schematic illustrations on the molecular arrangements of CN4OH/PVP (upper) and CN2OH/PVP (lower) blends in the presence of different amounts of PVP component.

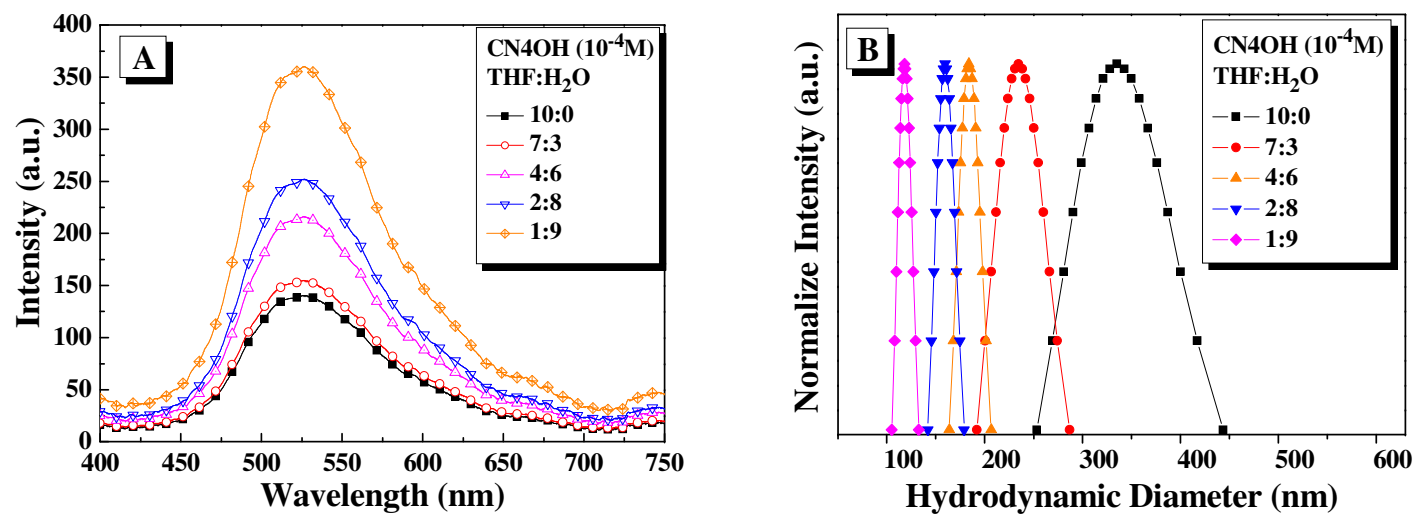


**Figure 1** (A) Solution emission spectra ( $\lambda_{\text{ex}} = 365 \text{ nm}$ ) and (B) histograms of hydrodynamic diameters of CN4OH in THF/water solvent mixtures containing different amounts of water.

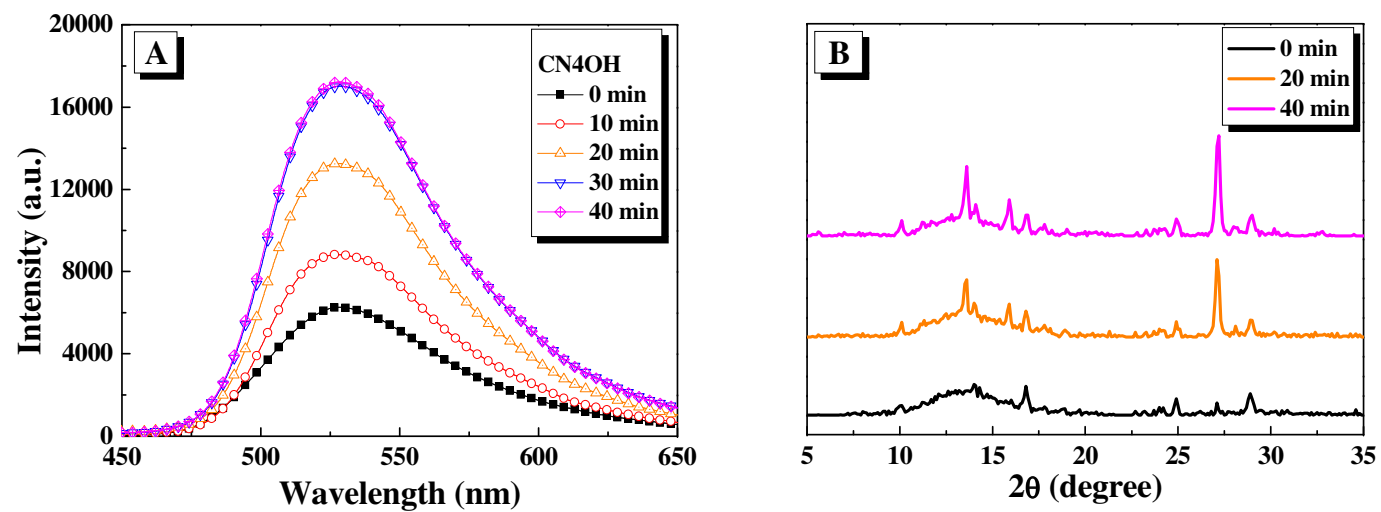


**Figure 2** (A) PL emission spectra ( $\lambda_{\text{ex}} = 365 \text{ nm}$ ) and (B) WAXD spectra of solid CN4OH after exposure to ethanol vapor for different time.

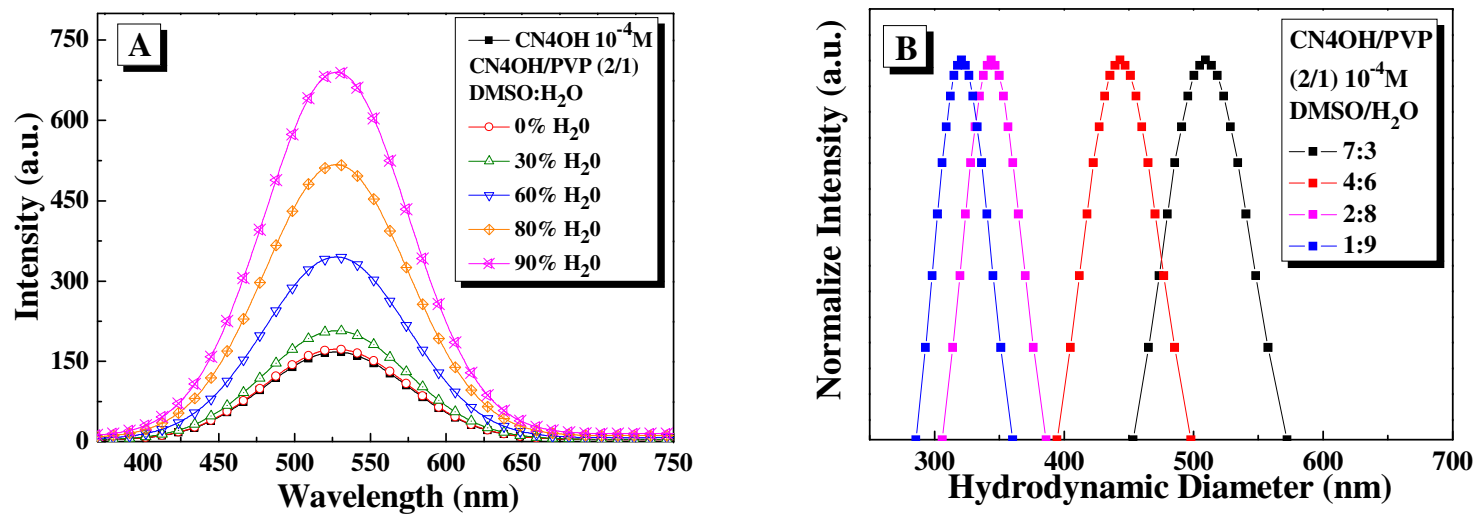


**Figure 3** (A) Solution emission spectra ( $\lambda_{\text{ex}} = 365$  nm) and (B) histograms of hydrodynamic diameters of CN4OH and CN4OH/PVP (2/1) mixtures in DMSO containing different amounts of water.

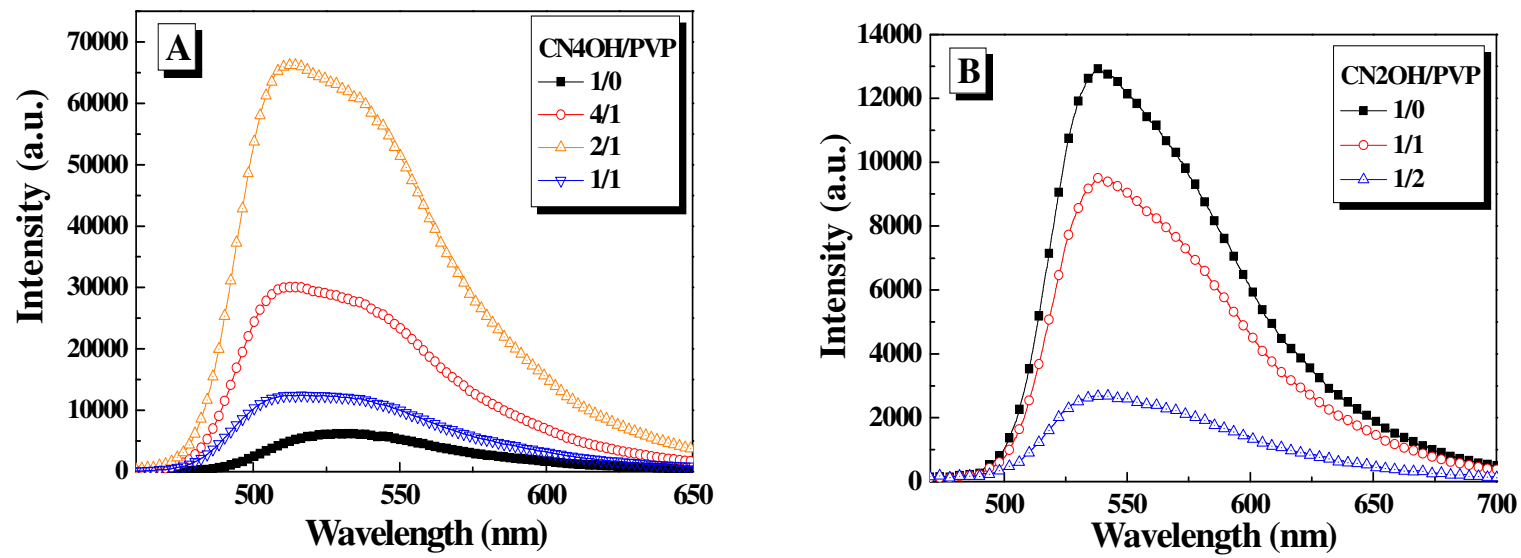


**Figure 4** Solid emission spectra of (A) CN4OH/PVP and (B) CN2OH/PVP blends.



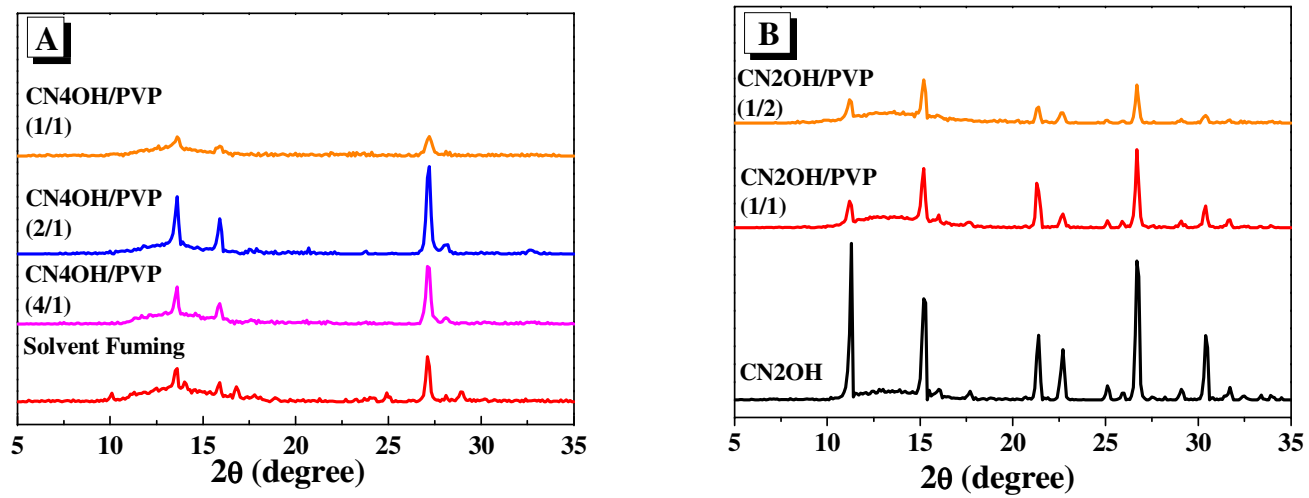


**Figure 5** WAXD spectra of (A) CN4OH/PVP blends and (B) CN2OH and CN2OH/PVP blends.